# FabF and FadM Cooperate to Recycle Fatty Acids and Rescue Δ*plsX* Lethality in *Staphylococcus aureus*

Paprapach Wongdontree[1], Milya Palmier[1], Vincent Leguillier[1], Clara Louche[1], Karine Gloux[1], David Halpern[1], Jamila Anba-Mondoloni[1], Alexandra Gruss[1#]

[1] Université Paris-Saclay, INRAE, AgroParisTech, Micalis Institute, 78350, Jouy-en-Josas, France.

[#] For correspondence: alexandra.gruss@inrae.fr

**Keywords:** *Staphylococcus aureus,* fatty acid, FASII, phospholipid synthesis, *plsX* deletion suppressors, FabF, FadM, acyl-CoA thioesterase, acyl-ACP thioesterase, ACP-binding, membrane.

**Short title:** FabF-FadM role in fatty acid recycling

**Abstract**

Phospholipids are essential components of most cell membranes. In *Staphylococcus aureus*, PlsX acyltransferase is considered indispensable for initiating phospholipid synthesis, unless exogenous fatty acids (FAs) are available for a bypass route. We report that *S. aureus* can capture internal FAs sources that overcome PlsX essentiality *via* gain-of-function mutations in two alleles: Δ*pls*X suppression by a FabF mutation, as mimicked by a FabF antibiotic inhibitor, suggests that FabF stalling causes FA release. Suppressor mutations in FadM, a bifunctional acyl-CoA thioesterase and ACP-binding protein, appear to retain only ACP-binding activity. The *fabF* and *fadM* suppressors compensate PlsX forward, but not reverse activity. Remarkably, *fabF* suppressors emerge only if *fadM* is present, indicative of FabF-FadM cooperation. We propose that increased ACP binding in FadM suppressor mutants facilitates FA release from FabF-acyl-ACP intermediates. A FabF-FadM relay leading to FA release may contribute to homeostasis between FASII and phospholipid synthesis pathways.

**Importance**

Phospholipids are vital cell membrane components. The *Staphylococcus aureus* PlsX enzyme uses acyl-ACP, the product of fatty acid (FA) synthesis (FASII), to initiate phospholipid production. Despite its central role, PlsX can be substituted by exogenous FAs whose phosphorylation yields the same product. We discovered that without FA supplementation, mutants arise that rescue growth, indicating that internal FAs are released. Mutations occurred in either FabF, a FASII enzyme, or in FadM, a little characterized protein. Our analyses give evidence that FabF and FadM proteins cooperate, and stimulate FA availability when either protein is mutated. We propose that in normal conditions, FadM acts as an "overflow valve" by releasing FAs from the FabF intermediate, which prevents buildup of FASII intermediates, and ensures FA-phospholipid balance.

## Introduction

Lipids provide the essential scaffolding for cell membranes and life. Bacterial phospholipid membranes comprise fatty acids (FA) that are attached to a glycerophosphate backbone (1). The phospholipid FAs are either produced by the FA synthesis (FASII) pathway or captured from the environment (2). The FASII product, acyl-Acyl Carrier Protein (acyl-ACP or FA-ACP) is a substrate for three enzymes: FabF for FA elongation *via* FASII, and PlsX and PlsC for respectively the first and second steps of phospholipid synthesis (**Fig. 1**).

The membrane-associated acyltransferase PlsX catalyzes the first dedicated step of phospholipid synthesis in Bacillota bacteria, by reversibly catalyzing conversion of acyl-ACP, the FASII product, to acyl-phosphate (acyl-$PO_4$) (3). An alternative phospholipid initiation mechanism, not requiring PlsX, involves assimilation of exogenous FAs *via* phosphorylation by the FA kinase Fak (4). The membrane glycerol-3-phosphate acyltransferase PlsY then transfers the FA moiety of acyl-$PO_4$ to the 1-position of the glycerophosphate backbone, forming lysophosphatidic acid. However, reverse PlsX activity may also reconvert acyl-$PO_4$ to acyl-ACP, which can then re-enter the FASII system or be used by PlsC for phospholipid synthesis (4, 5) (**Fig. 1**). Providing acyl-ACP by PlsX reverse activity on exogenous FAs, once phosphorylated, allows bacteria to overcome the need for FASII, making them insensitive to FASII inhibitors (6-8). In *Bacillus subtilis*, PlsX is membrane-associated for phospholipid synthesis, which could facilitate acyl-$PO_4$ transfer to PlsY, but likely not for its reverse activity (9). PlsX is thus a sorting station that initiates phospholipid synthesis, or returns acyl groups for FASII elongation and PlsC processing.

When exogenous FAs are absent, PlsX may still be dispensable in some bacteria. Numerous Pseudomonadota bacteria encode PlsB, which has functional redundancy to PlsX-PlsY (3). In *E. coli*, suppressors of the synthetic lethal Δ*plsX*Δ*plsY* mutation (despite the existence of the functionally redundant enzyme PlsB (3)) (10) displayed increased pools of glycerol-3-phosphate (Gly-3-P), the backbone for FA attachment to produce phospholipids (10). Increased Gly-3-P was suggested to compensate the low efficiency acyl-transferase activity of PlsB compared to PlsY. Among Bacillota pathogens, some deploy acyl-ACP thioesterases (acyl-ACP TEs) that liberate endogenous FAs from acyl-ACP**,** which are then phosphorylated by Fak to initiate phospholipid synthesis (11-14). Acyl-ACP TE fully restores growth of *Streptococcus pneumoniae* Δ*plsX* (12), and conditionally rescues *Enterococcus faecalis* Δ*plsX* growth; however, the acyl-ACP TE preferentially cleaves acyl-ACP comprising

unsaturated FAs, while growth is stimulated by saturated FAs (13). These alternative systems in Bacillota all generate an internal FA supply to initiate phospholipid synthesis when PlsX function is impaired.

The major human pathogen *Staphylococcus aureus* lacks an acyl-ACP TE to liberate FAs, and only exogenous FAs or a cloned heterologous acyl-ACP TE reportedly complemented growth of a *plsX* deletion strain (5). In this report, we characterized gain-of-function mutations mapping to two distinct loci that rescue Δ*plsX* viability without exogenous FAs. Mutations in FASII enzyme FabF, a 3-oxoacyl-ACP synthase II, or in a little characterized acyl-CoA thioesterase (acyl-CoA TE) and ACP binding protein designated as FadM, rescue Δ*plsX* growth. Our findings indicate that FadM and FabF cooperate, such that FA availability is increased when either protein is mutated. These findings suggest a general role for FadM in shuttling FAs from FASII towards phospholipid synthesis.

## Results

**Construction and confirmation of a Δ*plsX* in-frame mutant.** *plsX* is the second gene in a multicistronic operon also comprising FASII genes (**Fig. S1**). We constructed in-frame Δ*plsX* mutants of RN-R (RN4220 repaired for a defective *fakB1* gene in the 8325 lineage (15)) and of USA300_FPR3757 JE2 strains. Both Δ*plsX* mutants failed to grow on solid medium in the absence of FAs. Deletions were confirmed by PCR and whole genome sequencing (**Table S1**) and by RN-R Δ*plsX* growth complementation in the absence of FAs using a plasmid-carried copy of the intact *plsX* gene (**Fig. S2**).

**FA auxotrophy of *S. aureus* Δ*plsX* mutants is suppressed by a point mutation in *fabF*.** During phenotypic characterization of the purified confirmed JE2 Δ*plsX* mutant, we noted the appearance of colonies on BHI medium without FA (**Fig. 2A**, left plate). Two colonies subjected to whole genome sequencing confirmed the in-frame *plsX* deletion and also revealed point mutations mapping to FabF (SAUSA300_0886), the 3-oxoacyl-ACP synthase II of the FASII elongation cycle (see **Fig. 1**), producing $FabF^{A119E}$ (alanine to glutamic acid; Sup1) and $FabF^{D266A}$ (aspartic acid to alanine; Sup2). The suppressor carrying $FabF^{D266A}$ was not recoverable from the primary stocked strain, possibly because the mutation was deleterious for growth. Sup1 and Sup2 also carried the same point mutation in *csa1A* (SAUSA300_0100), encoding a tandem lipoprotein.

We expanded our analyses by isolating 31 other Δ*plsX* suppressors from RN-R or JE2 backgrounds (16 and 15 suppressors, respectively), and screened for those carrying *fabF* mutations by PCR followed by DNA sequence analyses (**Table S2**). Among them, 14 carried *fabF* mutations, which mapped to the same *fabF* nucleotide position in both strain backgrounds, resulting in a $FabF^{A119E}$ alteration as in Sup1. This allele is referred to as $fabF^{m}$. *csa1A*, which carried a mutation in Sup1 and Sup2 mutants, was not mutated in the 14 *fabF* mutants, indicating that *fabF* was the suppressor allele. Emergence of the same *fabF* mutation in both suppressor strain backgrounds could suggest that few FabF point modifications would allow both FASII activity and Δ*plsX* complementation.

Attempts to demonstrate the $fabF^{m}$ Δ*plsX* suppressor phenotype with a cloned *fabF* or $fabF^{m}$ allele were unsuccessful. A clone expressing $fabF^{m}$, but not WT *fabF* could be established in the WT RN-R strain by direct transformation; however, we failed to establish the $fabF^{m}$ clone in the Δ*plsX* background, even in FA-supplemented medium. This suggested that *fabF* overexpression was toxic in *S. aureus*, as reported in *Escherichia coli* (16).

As an alternate approach, we used a FabF inhibitor, platensimycin, to determine whether disabling FabF was responsible for Δ*plsX* suppression. This antibiotic binds to the acyl-ACP-FabF intermediate, and competes with malonyl-ACP entry, thus preventing FA elongation (17). We hypothesized that platensimycin could mimic the FabF suppressor mutation, and tested whether it would overcome the Δ*plsX* growth defect. RN-R Δ*plsX* cultures were plated on BHI solid medium, and platensimycin (1.5 µg) was deposited on plates then incubated 96 h at 37°C (**Fig. 2A**, right plate). In addition to the emergence of Δ*plsX* suppressors, a distinct homogeneous growth ring appeared around the platensimycin spots. Since the *fabF* mutants and a FabF inhibitor both restore Δ*plsX* growth, we consider it likely that the FabF mutation is directly responsible for Δ*plsX* suppression. Reducing *fabF* efficacy by mutation or platensimycin treatment could destabilize the FabF-acyl-ACP intermediate, to liberate free FAs and complement the Δ*plsX* growth defect (**Fig. 2B**).

**FA auxotrophy of *S. aureus* Δ*plsX* mutants is suppressed by mutations in *fadM* that disable the acyl-CoA binding cavity.** We searched for mutations that conferred Δ*plsX* growth on BHI among the 17 suppressors carrying a wild type *fabF* sequence. Genomic DNA sequencing was performed on three such isolates (one derived from RN-R Δ*plsX* and two from JE2 Δ*plsX* backgrounds). A single common gene target, SAOUHSC_01348 in RN-R or SAUSA300_1247 in JE2, was mutated (**Table S1**, **Table S2**). While annotated as a DHNA thioesterase, the target protein was shown to have acyl-CoA TE activity (18). Moreover, the 155-amino-acid ORF

shares ~40% similarity and a conserved serine, histidine and aspartic acid catalytic triad with FadM, an *E. coli* acyl-CoA TE and ACP-binding protein (PBD database protein 1NJK), (18-22). The *S. aureus* gene, referred to as *fadM*, was PCR-amplified and sequenced in the 17 other suppressors lacking mutations in *fabF*. All carried mutations in *fadM*. A single variant (encoding FadM$^{Y90F}$, [*fadM*$^{m2}$]) was identified in the four isolates selected from RN-R Δ*plsX*; three distinct FadM variants were identified among the JE2 Δ*plsX* suppressors (FadM$^{I38T}$ [*fadM*$^{m1}$], FadM$^{Y90F}$ [*fadM*$^{m2}$], and FadM$^{Y133F}$ [*fadM*$^{m3}$]) (**Table S1**, **Table S2**). These results point to FabF and FadM as the main mutational suppressors rescuing Δ*plsX* growth.

The *S. aureus* FadM crystal structure (PDB: 6FDG) and Alphafold design (https://alphafold.ebi.ac.uk/entry/A0A0H2XFE3) were used to map the three identified FadM mutations conferring Δ*plsX* suppression. The mutations coincided with or mapped adjacent to amino acids reportedly involved in forming an FA binding cavity that favors long FA substrates (18) (**Fig. 3A**). The grouped location of these mutations suggests that acyl-CoA TE activity is defective in the FadM suppressor mutants.

A positive role for acyl-CoA TE in Δ*plsX* suppression is further ruled out: The FadM TE substrate, acyl-CoA, is synthesized by acyl-CoA synthetase (encoded by *fadE* in *S. aureus*, which is part of the fatty acid degradation (*fad*) system (23, 24)). If FadM acyl-CoA TE were needed for Δ*plsX* suppression, acyl-CoA would first have to be produced by FadE. The *fad* genes are subject to CcpA-mediated glucose repression (24, 25). However, glucose did not affect the *fadM*$^{m}$ Δ*plsX* suppressor phenotypes (**Fig. S3**). Based on above results, we conclude that acyl-CoA TE activity is not responsible for Δ*plsX* rescue.

**FadM inactivation abolishes Δ*plsX* suppression.** Suppression by *fadM* mutants could be due to FadM-mediated ACP-binding, or to the loss of FadM altogether. We asked whether inactivation of *fadM*, the downstream gene in a 2-gene operon comprising *acnA* ((26); **Fig. S1**), suppresses the Δ*plsX* phenotype. For this, *fadM* was inactivated by transducing a *fadM* transposon insertion, interrupting FadM at amino acid position 5, from the NARSA library into the JE2 Δ*plsX fadM*$^{m2}$ suppressor (strain 7.1; **Table S2**) (25). The Δ*plsX fadM*::Tn strain failed to grow on FA-free medium (**Fig. 3B**). Since total loss of FadM does not promote Δ*plsX* suppression, we conclude that FadM ACP binding activity is required for *S. aureus* Δ*plsX* suppression. The need for FadM but not its acyl-CoA TE activity strongly suggests that FadM ACP binding activity confers Δ*plsX* suppression (**Fig. 3C**).

**Membrane FAs are altered in *fabF* and *fadM* suppressors of Δ*plsX*.** We assessed membrane FA composition of Δ*plsX* suppressors in RN-R and JE2 backgrounds in medium devoid of FAs (**Fig. 4A**, **Table S3**). The *fabF* suppressor strains produced membrane FAs of markedly shorter overall length in both strain backgrounds. Notably, straight-chain FAs C18:0 and C20:0, represent 20-30% of total FAs in parental strains but are essentially absent in *fabF* suppressors. This could be explained if the mutated $FabF^{A119E}$ suppressor allele is partially defective for elongating the acyl-ACP substrate. In *S. aureus*, branched chain precursors are preferred substrates for FabH (see **Fig. 1**; (27)), which might lead to higher proportions of branched chain FAs in $fabF^{m}$ suppressors. FA profiles in $fadM^{m}$ suppressor strains were less drastically affected, but nevertheless showed a 2-fold decrease in proportions of C18:0 and C20:0 compared to those in the respective parental strains (**Table S3**). These results confirm that Δ*plsX* $fabF^{m}$ and Δ*plsX* $fadM^{m}$ suppressors diminish the proportion of long chain saturated FAs in phospholipids.

**Acyl-ACP species variation in JE2 WT, Δ*plsX*, and Δ*plsX* suppressors.** Acyl-ACP accumulates in a *plsX* deletion strain, since the next step, in which PlsC uses acyl-ACP to produce phosphatidic acid, cannot proceed until position 1 of the glycerophosphate backbone is occupied (**Fig. 1**; (5, 28)). We assessed acyl-ACP intermediate accumulation in the JE2 Δ*plsX* mutant and derivative suppressors by non-denaturing polyacrylamide gel electrophoresis, and hybridization with anti-ACP antibodies (7, 29) (**Fig. 4B**). Unlike the WT strain, the Δ*plsX* mutant was distinguished by the presence of a fast-migrating band corresponding to ACP bound to long-chain FAs. In contrast, the long acyl-ACP species was absent in both Δ*plsX* $fabF^{m}$ and Δ*plsX* $fadM^{m}$ suppressors, indicating that acyl-ACP is processed to initiate phospholipid synthesis. The reasonable conclusion is that both *fabF* and *fadM* suppressor strains release endogenous FAs to bypass Δ*plsX* synthesis inhibition.

**Impact of Δ*plsX* suppressors on bacterial growth.** Growth of Δ*plsX* suppressors was assessed in RN-R and JE2 backgrounds in non-FA-supplemented BHI medium (**Fig. 4C**). The initial Δ*plsX* deletion strains fail to grow unless supplemented with FAs. Both *fabF* and *fadM* suppressor mutants grew similarly, but their growth phenotypes differed according to the parental strains: in the RN-R background, growth of both tested suppressors was intermediate between the WT strain and the Δ*plsX* mutant. In contrast, JE2 derivative suppressors grew like the parental strain. A distinguishing feature between the two *S. aureus* strains is the production of staphyloxanthin pigment by JE2 but not by RN-R (an RN4220 derivative). The

hydrophobic long-chain isoprenyl moiety of staphyloxanthin (30) might contribute to JE2 survival by stabilizing the membrane in suppressor strains with shorter FAs. This hypothesis remains to be tested. Thus, both *fabF* and *fadM* suppressor phenotypes restore overall bacterial fitness to Δ*plsX*, particularly in the JE2 background.

**Δ*plsX* suppressors do not compensate reverse PlsX activity, which is required to bypass the FASII pathway.** We asked whether *fabF* and/or *fadM* suppressor strains could complement the reverse PlsX activity, i.e., conversion of acyl-$PO_4$ to acyl-ACP (**Fig. 5** left). If this were the case, FASII inhibition in suppressors would be bypassed by FA supplementation to growth medium. To test this, WT strain JE2, and isogenic Δ*plsX*, Δ*plsX fabF*$^m$, and Δ*plsX fadM*$^m$ strains were grown in medium containing FAs (SerFA), without and with the FASII inhibitor AFN-1252 (31) (**Fig. 5** right). All strains grew to equivalent densities in the absence of inhibitor. The JE2 WT strain overcame the presence of AFN-1252 in SerFA (6, 8). In contrast, neither the Δ*plsX* mutant nor the Δ*plsX* suppressors could bypass the FASII inhibitor. These findings show that *fabF* or *fadM* suppressor mutations do not compensate the PlsX reverse reaction, and that FASII must be active for Δ*plsX* suppressor growth.

**Evidence that FabF and FadM have cooperative roles in Δ*plsX* growth rescue.** As *fadM* interruption abolished Δ*plsX* suppression (**Fig. 3**), we reasoned that suppressors arising in the Δ*plsX fadM*::Tn mutant would map to *fabF*. This hypothesis was tested by comparing suppressor emergence in JE2 Δ*plsX* and Δ*plsX fadM*::Tn mutants on solid medium without FA supplementation. We simultaneously tested for a stimulatory effect of the FabF inhibitor platensimycin as seen for the Δ*plsX* mutant (**Fig. 6**). Unexpectedly, no suppressors arose after extended (> 1 week) plate incubation at 37°C, compared to frequent mutant emergence in the Δ*plsX* background after 1-2 days. Moreover, no stimulatory growth ring was detected surrounding the platensimycin. These results affirm that intact FadM, whether wild type or mutated, is required to obtain FabF suppression of Δ*plsX*. We conclude that FabF and FadM interact in the same pathway.

**Conclusions**

This study shows that PlsX, which is reportedly required for *S. aureus* growth in the absence of exogenous FAs, can be compensated by gain-of-function mutations in either FabF or in a little-characterized bi-functional protein, FadM, with reported acyl-CoA thioesterase and ACP binding activity (18, 21). Here we identified a previously unknown cooperative link between

FabF and FadM that adds FadM among the factors implicated in *S. aureus* FASII and phospholipid homeostasis. We propose a model in which FadM facilitates ACP removal from the acyl-ACP-FabF intermediate, prior to malonyl-ACP entry (32) (**Fig. 9**): the $FabF^{A119E}$ mutant rescues Δ*plsX* by releasing its FA cargo just before malonyl-ACP entry. FadM binding to ACP would facilitate ACP removal from the FabF cavity, thus favoring FA liberation for its phosphorylation, and subsequent entry into the phospholipid synthesis pathway. Our results indicate that FadM suppressor mutations occlude the FA-binding cavity, which disables acyl-CoA TE activity (**Fig. 3A**). In consequence, more FadM would be available for ACP binding to the FabF intermediate. Thus, either FabF stalling at an intermediate step, or more efficient FadM-mediated removal of ACP from the FabF-acyl-ACP intermediate, would increase FA release by FabF. Mutants lacking FadM would be unable to release FA from the FabF intermediates, explaining the lack of suppressors in the Δ*plsX fadM*::Tn background (**Fig. 7**). FadM could also contribute to FASII-phospholipid homeostasis in WT *S. aureus*, by acting as an FA release valve that decreases FabF processivity, leading to shortened phospholipid FAs in stress conditions.

## Materials and methods

**Strains, growth conditions, and plasmids.** Strains and plasmids are listed in **Table S4**. *S. aureus* strains are derived from USA300_FPR3757 strain JE2 (25) and RN4220-R (called here RN-R; (15)). RN-R is a readily transformable strain derived from RN4220, of the NCTC 8325 lineage (33). It was repaired to restore a functional *fakB1* gene, which is defective in the entire NCTC 8325 lineage (15)). *S. aureus* parental strains and Δ*plsX*-suppressor mutants were grown in BHI medium (Brain Heart Infusion; Gibco, France) or in LB as specified, at 37°C with shaking. Medium was supplemented with C18:1 (oleic acid) at a concentration of 250 µM (Larodan, Sweden) when indicated. The FabI inhibitor AFN-1252 (Med ChemExpress, France) and FabF inhibitor platensimycin (Bioaustralis-Tebubio France) were used as specified (17, 34).

**Δ*plsX* mutant construction.** The Δ*plsX* mutants were constructed in RN-R (RN4220 repaired for a defective *fakB1* gene in the NCTC8325 lineage; (15)) and JE2 backgrounds. The preparatory plasmid for *plsX* deletion was constructed using the Gibson assembly method to insert DNA segments flanking the *plsX orf* into Sma1-linearized pMAD, a thermosensitive plasmid expressing erythromycin resistance (35, 36). Oligonucleotides for Δ*plsX* construction are in **Table S5**. Constructions were verified by DNA sequencing of PCR-amplified fragments. The double cross-over gene replacements were obtained as described (15, 36) in RN-R and JE2 strains. Deletions removed nucleotides 1,228,616-1,229,594 in JE2, and 1,148,670-1,149,648 in RN-R, as per respective annotated genomes. The resultant strain genotypes were confirmed by whole genome sequencing (Eurofins, Germany).

***plsX* cloning and complementation of the Δ*plsX* mutant in RN-R and JE2 strains.** To confirm that strain characteristics were due to the *plsX* deletion, the intact *plsX* gene was cloned with its natural promoter (upstream of *fapR*) on multicopy plasmid pIM-locus1 (a pIMAY derivative (37, 38)). Cloning was performed by Gibson assembly with oligonucleotide primers (**Table S5**).

**Isolation of suppressor mutants.** RN-R Δ*plsX* and JE2 Δ*plsX* strains were first streaked on solid BHI medium containing 250 µM C18:1, an FA that promotes growth. For each strain, a single colony was used to inoculate a liquid culture (in BHI+C18:1). When the culture reached exponential phase, bacteria were centrifuged, resuspended in BHI, and adjusted to $OD_{600}$ = 0.1. Dilutions were plated on solid medium to obtain ~$10^5$ to ~$10^7$ colony forming units per plate on solid BHI medium without FAs. Colonies were scored after two or more days of

incubation at 37°C, and selected at random for restreaking on solid BHI medium. Liquid cultures were prepared in BHI, and stocked in 20% glycerol for storage at -70°C. Selected mutant genotypes were confirmed by whole genome sequencing or by PCR fragment sequencing (Eurofins, Germany) to identify mutated loci.

**Genomic DNA preparation for whole genome sequencing.** Bacterial cell pellets, prepared from 3 mL liquid exponential phase cultures, were centrifuged at 8,000 rpm for 5 min. Pellets were re-suspended in 800 µL Tris-EDTA buffer (10 mM Tris- HC1, pH 8.0/1 mM EDTA) plus 20 µL lysostaphin 5 mg/mL, and incubated for 45 min at 37°C. DNA was prepared by DNeasy Blood & Tissue Kit (Qiagen, France) and samples were outsourced for whole genome DNA sequencing using 2x150 bp paired end chemistry and bioinformatics analyses (Eurofins Genomics, France) (6). SNPs that differed in non-antibiotic-treated JE2 and RN-R strains from those in the reference sequence (GenBank Nucleotide accession codes NC_007793.1 and NC_007795.1 respectively) were subtracted prior to variant identification. Variants were identified as representing ≥80% of reads in sequences for which there were at least 100 reads.

**PCR amplification and confirmation by DNA sequencing.** Selected candidate colonies were suspended in 100 µL of 0.9% NaCl with 1 µL of lysostaphin from a 5 mg/mL stock. Tubes containing suspensions were shaken for 45 min at 37°C. Contents were then transferred to tubes containing glass beads and samples were vortexed for 1 min. After a 30 second centrifugation at 8000 rpm, PCR amplification was performed on 1 µl of supernatant, using primers (**Table S5**) and Phusion DNA polymerase (ThermoFisher Scientific, France) according to manufacturer protocol, using a SimpliAmp Thermal Cycler (ThermoFisher Scientific, France). PCR products were analyzed on a 0.8% agarose gel prepared in 40 mM Tris acetate 1 mM EDTA buffer containing 0.5 µg/mL ethidium bromide. Gels were run at 100 V for 30 min in an electrophoresis chamber (Mupid ONE; Dutscher, France), and photographed under UV light using the EBOX VX5 imaging system (Vilber Lourmat, France). PCR samples were purified using the NucleoSpin® Gel and PCR Clean-up kit (Macherey-Nagel, France), and sent for DNA sequencing (Eurofins, France).

**Effects of the FabF inhibitor platensimycin on Δ*plsX* and Δ*plsX fadM*::Tn strains.** Strains were grown in BHI containing C18:1 (250 µM) overnight, washed once in BHI medium, and resuspended in BHI to a final density of $OD_{600}$ = 0.1. From this, 100 µl of the bacterial suspension was plated on solid BHI medium. Platensimycin (1.5 µg in 3 µl) was spotted in the center of plates, which were then incubated at 37°C for 4-7 days and photographed.

**Effect of glucose on growth of Δ*plsX* suppressors.** Strains were precultured in liquid LB (n.b., LB lacks glucose) or LB with C18:1 for Δ*plsX* at 37°C. After overnight growth, cultures were diluted to $OD_{600}$ = 0.05 and grown for 3-4 hours. Δ*plsX* cultures were first centrifuged and resuspended in fresh LB medium to remove free FAs prior to regrowth. Bacterial densities were then adjusted to $OD_{600}$ = 1. Cultures were streaked on solid medium, corresponding to LB or LB containing 0.5% glucose, which represses *fad* operon expression (24, 26). Plates were incubated at 37°C for 24 hours and photographed.

**Growth kinetics.** Three mL precultures were prepared in BHI for parental and Δ*plsX* suppressor strains, or in BHI containing 250 µM C18:1 for Δ*plsX* mutants. After overnight growth, culture $OD_{600}$ were adjusted to $OD_{600}$ = 0.05 in 200 µL BHI medium without or with C18:1 (250 µM), in 96-well microtiter plates. Growth was followed on a Spark M10 plate reader (Tecan, France). For experiments in which samples were taken for FA determinations or for Western blot experiments, cultures were prepared in 3 to 10 ml liquid cultures, and were monitored manually by $OD_{600}$ measurements every two hours.

**Determination of membrane FA profiles.** Bacterial cultures (equivalent of $OD_{600}$ = 2) were centrifuged, and pellets were washed once in 1 ml of 0.02% Triton in 0.9% NaCl, then twice with 1 ml of 0.9% NaCl. FA extractions were performed as described (6).

**Detection of ACP products.** Pellets from $OD_{600}$=10 equivalent of exponential phase cultures were collected by centrifugation (8000 rpm for 5 min), and then washed twice with PBS (Phosphate Buffer Saline)-Triton X100 0.1%, and once with PBS. Pellets were re-suspended in 600 µL PBS supplemented with 6 µL antiprotease (100X), 50 µg/mL lysostaphin and 50 µg/mL DNAse and incubated with shaking for 25 min at 37°C. Protein concentrations were determined (39), and extracts (10 µg) were loaded onto non-denaturing gels containing 1M urea and 14% acrylamide gel as described (5, 7). After electrophoresis, gels were subject to electroblotting for transfer to a PVDF membrane (Biorad, France) using a current of 25 V and 1.3 A on a power blotter semi-dry transfer system (Invitrogen, France) for 7 min. Primary anti-ACP antibody (Covalabs, France; (7)) was used at 1:500 dilution and secondary anti-rabbit IgG conjugated with peroxidase (Invitrogen, France) at a 1:5000 dilution. ACP-reactive bands were identified using the ECL kit (Perkin Elmer, France) and the fluorescent signal was recorded using ChemiDoc (BioRad, France).

**Phage transduction.** Transduction of transposon insertions from JE2 into Δ*plsX* mutant backgrounds was performed as described using ϕ80 phage stock (40). The *fadM* transposon insertion (25) was transduced into JE2 Δ*plsX fadM*$^{m2}$ suppressor strain 7.1, giving rise to Δ*plsX fadM*::Tn, by selecting for erythromycin (5 µg/ml) (**Table S4**). Insertion was confirmed by PCR.

**FASII bypass of WT and Δ*plsX* derivative strains.** Anti-FASII bypass was evaluated as described (6). Strains were grown overnight in liquid SerFA medium (SerFA, BHI containing 10 % newborn calf serum and an equimolar mixture of 85 µM each C14:0, C16:0, and C18:1 [Larodan, Sweden]). Cultures were then diluted to $OD_{600}$=0.05 in SerFA containing or not the anti-FASII AFN-1252 (here called AFN; (31); MedChemExpress, France). Growth was monitored using the Spark plate reader (Tecan, France).

**Acknowledgements and funding**

We are grateful to Kam Pou Han and Philippe Bouloc (Bouloc lab, I2BC, Orsay, France) for providing transducing phage and plasmid; Florence Dubois-Brissonet and Katia de Oliveira (Micalis, INRAE) for expert help and advice with CpG analyses; Olivier Son for help with phage transduction. We thank Micalis Institute colleagues Vincent Juillard for discussion of PlsX functions, and Philippe Gaudu and team members for stimulating discussion and pertinent comments.

This work was supported by the French Agence Nationale de la Recherche ANR (ANR-16-CE15-0013; AG), the Joint Programming Initiative on Antimicrobial Resistance (JPIAMR) under the umbrella of the ANR (ANR-22-AAMR-0007; AG), and the Fondation pour la Recherche Medicale (DBF20161136769; AG). PW was recipient of a Franco-Thai scholarship from Campus France and Khon Kaen University.

**Data availability**

All relevant data are within the manuscript, supporting information files, and repositories. Any biological materials are available upon request.

**Author Contributions**

All authors performed, analyzed, and interpreted experiments, and approved the manuscript. PW, JAM, and AG conceived the project, designed research, and wrote the paper.

**Competing interests**

The authors declare no competing interests.

**References**


1. Zhang YM, Rock CO. 2008. Membrane lipid homeostasis in bacteria. Nat Rev Microbiol 6:222-33.
2. Silbert DF, Ruch F, Vagelos PR. 1968. Fatty acid replacements in a fatty acid auxotroph of *Escherichia coli*. J Bacteriol 95:1658-65.
3. Lu YJ, Zhang YM, Grimes KD, Qi J, Lee RE, Rock CO. 2006. Acyl-phosphates initiate membrane phospholipid synthesis in Gram-positive pathogens. Mol Cell 23:765-72.
4. Parsons JB, Broussard TC, Bose JL, Rosch JW, Jackson P, Subramanian C, Rock CO. 2014. Identification of a two-component fatty acid kinase responsible for host fatty acid incorporation by *Staphylococcus aureus*. Proc Natl Acad Sci U S A 111:10532-7.
5. Parsons JB, Frank MW, Jackson P, Subramanian C, Rock CO. 2014. Incorporation of extracellular fatty acids by a fatty acid kinase-dependent pathway in *Staphylococcus aureus*. Mol Microbiol 92:234-45.
6. Kenanian G, Morvan C, Weckel A, Pathania A, Anba-Mondoloni J, Halpern D, Gaillard M, Solgadi A, Dupont L, Henry C, Poyart C, Fouet A, Lamberet G, Gloux K, Gruss A. 2019. Permissive Fatty Acid Incorporation Promotes Staphylococcal Adaptation to FASII Antibiotics in Host Environments. Cell Rep 29:3974-3982 e4.
7. Morvan C, Halpern D, Kenanian G, Hays C, Anba-Mondoloni J, Brinster S, Kennedy S, Trieu-Cuot P, Poyart C, Lamberet G, Gloux K, Gruss A. 2016. Environmental fatty acids enable emergence of infectious *Staphylococcus aureus* resistant to FASII-targeted antimicrobials. Nat Commun 7:12944.
8. Wongdontree P, Millan-Oropeza A, Upfold J, Lavergne JP, Halpern D, Lambert C, Page A, Kenanian G, Grangeasse C, Henry C, Fouet A, Gloux K, Anba-Mondoloni J, Gruss A. 2024. Oxidative stress is intrinsic to staphylococcal adaptation to fatty acid synthesis antibiotics. iScience 27:109505.
9. Sastre DE, Pulschen AA, Basso LGM, Benites Pariente JS, Marques Netto CGC, Machinandiarena F, Albanesi D, Navarro M, de Mendoza D, Gueiros-Filho FJ. 2020. The phosphatidic acid pathway enzyme PlsX plays both catalytic and channeling roles in bacterial phospholipid synthesis. J Biol Chem 295:2148-2159.
10. Rex AN, Simpson BW, Bokinsky G, Trent MS. 2024. PlsX and PlsY: Additional roles beyond glycerophospholipid synthesis in Gram-negative bacteria. mBio doi:10.1128/mbio.02969-24:e0296924.
11. Jing F, Cantu DC, Tvaruzkova J, Chipman JP, Nikolau BJ, Yandeau-Nelson MD, Reilly PJ. 2011. Phylogenetic and experimental characterization of an acyl-ACP thioesterase family reveals significant diversity in enzymatic specificity and activity. BMC Biochem 12:44.
12. Parsons JB, Frank MW, Eleveld MJ, Schalkwijk J, Broussard TC, de Jonge MI, Rock CO. 2015. A thioesterase bypasses the requirement for exogenous fatty acids in the *plsX* deletion of *Streptococcus pneumoniae*. Mol Microbiol 96:28-41.
13. Zou Q, Dong H, Cronan JE. 2023. Growth of *Enterococcus faecalis* Δ*plsX* strains is restored by increased saturated fatty acid synthesis. mSphere 8:e0012023.
14. Cross B, Garcia A, Faustoferri R, Quivey RG. 2016. PlsX deletion impacts fatty acid synthesis and acid adaptation in *Streptococcus mutans*. Microbiology (Reading) 162:662-671.
15. Pathania A, Anba-Mondoloni J, Gominet M, Halpern D, Dairou J, Dupont L, Lamberet G, Trieu-Cuot P, Gloux K, Gruss A. 2021. (p)ppGpp/GTP and Malonyl-CoA Modulate *Staphylococcus aureus* Adaptation to FASII Antibiotics and Provide a Basis for Synergistic Bi-Therapy. mBio 12.
16. Subrahmanyam S, Cronan JE, Jr. 1998. Overproduction of a functional fatty acid biosynthetic enzyme blocks fatty acid synthesis in *Escherichia coli*. J Bacteriol 180:4596-602.

17. Wang J, Soisson SM, Young K, Shoop W, Kodali S, Galgoci A, Painter R, Parthasarathy G, Tang YS, Cummings R, Ha S, Dorso K, Motyl M, Jayasuriya H, Ondeyka J, Herath K, Zhang C, Hernandez L, Allocco J, Basilio A, Tormo JR, Genilloud O, Vicente F, Pelaez F, Colwell L, Lee SH, Michael B, Felcetto T, Gill C, Silver LL, Hermes JD, Bartizal K, Barrett J, Schmatz D, Becker JW, Cully D, Singh SB. 2006. Platensimycin is a selective FabF inhibitor with potent antibiotic properties. Nature 441:358-61.
18. Murad AM, Brognaro H, Falke S, Lindner J, Perbandt M, Mudogo C, Schubert R, Wrenger C, Betzel C. 2022. Structure and activity of the DHNA Coenzyme-A Thioesterase from *Staphylococcus aureus* providing insights for innovative drug development. Sci Rep 12:4313.
19. Swarbrick CMD, Nanson JD, Patterson EI, Forwood JK. 2020. Structure, function, and regulation of thioesterases. Prog Lipid Res 79:101036.
20. Butland G, Peregrin-Alvarez JM, Li J, Yang W, Yang X, Canadien V, Starostine A, Richards D, Beattie B, Krogan N, Davey M, Parkinson J, Greenblatt J, Emili A. 2005. Interaction network containing conserved and essential protein complexes in *Escherichia coli*. Nature 433:531-7.
21. Cherkasov A, Hsing M, Zoraghi R, Foster LJ, See RH, Stoynov N, Jiang J, Kaur S, Lian T, Jackson L, Gong H, Swayze R, Amandoron E, Hormozdiari F, Dao P, Sahinalp C, Santos-Filho O, Axerio-Cilies P, Byler K, McMaster WR, Brunham RC, Finlay BB, Reiner NE. 2011. Mapping the protein interaction network in methicillin-resistant *Staphylococcus aureus*. J Proteome Res 10:1139-50.
22. Gully D, Bouveret E. 2006. A protein network for phospholipid synthesis uncovered by a variant of the tandem affinity purification method in *Escherichia coli*. Proteomics 6:282-93.
23. Fujita Y, Matsuoka H, Hirooka K. 2007. Regulation of fatty acid metabolism in bacteria. Mol Microbiol 66:829-39.
24. Kuiack RC, Tuffs SW, Dufresne K, Flick R, McCormick JK, McGavin MJ. 2023. The fadXDEBA locus of *Staphylococcus aureus* is required for metabolism of exogenous palmitic acid and in vivo growth. Mol Microbiol 120:425-438.
25. Fey PD, Endres JL, Yajjala VK, Widhelm TJ, Boissy RJ, Bose JL, Bayles KW. 2013. A genetic resource for rapid and comprehensive phenotype screening of nonessential *Staphylococcus aureus* genes. MBio 4:e00537-12.
26. Mader U, Nicolas P, Depke M, Pane-Farre J, Debarbouille M, van der Kooi-Pol MM, Guerin C, Derozier S, Hiron A, Jarmer H, Leduc A, Michalik S, Reilman E, Schaffer M, Schmidt F, Bessieres P, Noirot P, Hecker M, Msadek T, Volker U, van Dijl JM. 2016. *Staphylococcus aureus* Transcriptome Architecture: From Laboratory to Infection-Mimicking Conditions. PLoS Genet 12:e1005962.
27. Qiu X, Choudhry AE, Janson CA, Grooms M, Daines RA, Lonsdale JT, Khandekar SS. 2005. Crystal structure and substrate specificity of the beta-ketoacyl-acyl carrier protein synthase III (FabH) from *Staphylococcus aureus*. Protein Sci 14:2087-94.
28. Machinandiarena F, Nakamatsu L, Schujman GE, de Mendoza D, Albanesi D. 2020. Revisiting the coupling of fatty acid to phospholipid synthesis in bacteria with FapR regulation. Mol Microbiol 114:653-663.
29. Cronan JE, Thomas J. 2009. Bacterial fatty acid synthesis and its relationships with polyketide synthetic pathways. Methods Enzymol 459:395-433.
30. Pelz A, Wieland KP, Putzbach K, Hentschel P, Albert K, Gotz F. 2005. Structure and biosynthesis of staphyloxanthin from *Staphylococcus aureus*. J Biol Chem 280:32493-8.
31. Karlowsky JA, Kaplan N, Hafkin B, Hoban DJ, Zhanel GG. 2009. AFN-1252, a FabI inhibitor, demonstrates a Staphylococcus-specific spectrum of activity. Antimicrob Agents Chemother 53:3544-8.
32. Mindrebo JT, Patel A, Kim WE, Davis TD, Chen A, Bartholow TG, La Clair JJ, McCammon JA, Noel JP, Burkart MD. 2020. Gating mechanism of elongating beta-ketoacyl-ACP synthases. Nat Commun 11:1727.

33. Herbert S, Ziebandt AK, Ohlsen K, Schafer T, Hecker M, Albrecht D, Novick R, Gotz F. 2010. Repair of global regulators in *Staphylococcus aureus* 8325 and comparative analysis with other clinical isolates. Infect Immun 78:2877-89.
34. Hunt T, Kaplan N, Hafkin B. 2016. Safety, tolerability and pharmacokinetics of multiple oral doses of AFN-1252 administered as immediate release (IR) tablets in healthy subjects. J Chemother 28:164-71.
35. Arnaud M, Chastanet A, Debarbouille M. 2004. New vector for efficient allelic replacement in naturally nontransformable, low-GC-content, gram-positive bacteria. Appl Environ Microbiol 70:6887-91.
36. Biswas I, Gruss A, Ehrlich SD, Maguin E. 1993. High-efficiency gene inactivation and replacement system for gram-positive bacteria. J Bacteriol 175:3628-35.
37. Coronel-Tellez RH, Pospiech M, Barrault M, Liu W, Bordeau V, Vasnier C, Felden B, Sargueil B, Bouloc P. 2022. sRNA-controlled iron sparing response in Staphylococci. Nucleic Acids Res 50:8529-8546.
38. Monk IR, Shah IM, Xu M, Tan MW, Foster TJ. 2012. Transforming the untransformable: application of direct transformation to manipulate genetically *Staphylococcus aureus* and Staphylococcus epidermidis. mBio 3.
39. Bradford MM. 1976. A rapid and sensitive method for the quantitation of microgram quantities of protein utilizing the principle of protein-dye binding. Anal Biochem 72:248-54.
40. Bowring JZ, Su Y, Alsaadi A, Svenningsen SL, Parkhill J, Ingmer H. 2022. Screening for Highly Transduced Genes in *Staphylococcus aureus* Revealed Both Lateral and Specialized Transduction. Microbiol Spectr 10:e0242321.
41. Brown ED. 2006. Microbiology: antibiotic stops 'ping-pong' match. Nature 441:293-4.
42. Jumper J, Evans R, Pritzel A, Green T, Figurnov M, Ronneberger O, Tunyasuvunakool K, Bates R, Zidek A, Potapenko A, Bridgland A, Meyer C, Kohl SAA, Ballard AJ, Cowie A, Romera-Paredes B, Nikolov S, Jain R, Adler J, Back T, Petersen S, Reiman D, Clancy E, Zielinski M, Steinegger M, Pacholska M, Berghammer T, Bodenstein S, Silver D, Vinyals O, Senior AW, Kavukcuoglu K, Kohli P, Hassabis D. 2021. Highly accurate protein structure prediction with AlphaFold. Nature 596:583-589.
43. Pettersen EF, Goddard TD, Huang CC, Couch GS, Greenblatt DM, Meng EC, Ferrin TE. 2004. UCSF Chimera--a visualization system for exploratory research and analysis. J Comput Chem 25:1605-12.
44. Brinster S, Lamberet G, Staels B, Trieu-Cuot P, Gruss A, Poyart C. 2009. Type II fatty acid synthesis is not a suitable antibiotic target for Gram-positive pathogens. Nature 458:83-6.
45. Monk IR, Stinear TP. 2021. From cloning to mutant in 5 days: rapid allelic exchange in *Staphylococcus aureus*. Access Microbiol 3:000193.
46. Christie GE, Matthews AM, King DG, Lane KD, Olivarez NP, Tallent SM, Gill SR, Novick RP. 2010. The complete genomes of *Staphylococcus aureus* bacteriophages 80 and 80alpha--implications for the specificity of SaPI mobilization. Virology 407:381-90.

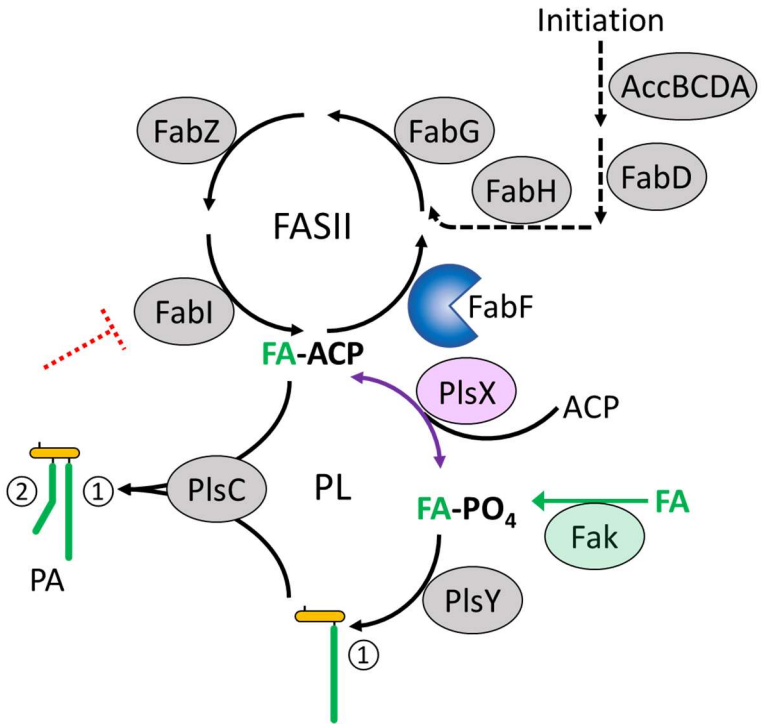


**Fig. 1: Roles of the reversible PlsX enzyme in phospholipid synthesis.** The FASII pathway schematized here produces acyl-ACP (FA-ACP), which may either be elongated by FASII using FabF (blue), or used by PlsX (purple) to initiate phospholipid (PL) synthesis. The PlsX product FA-$PO_4$ is a substrate for PlsY, a membrane protein that joins the acyl group to the glycerophosphate backbone in position 1 (①, bottom). PlsC uses this intermediate product (lysophosphatidic acid), to add the second acyl moiety from FA-ACP to position 2 (②), generating phosphatidic acid (PA, left). Reverse PlsX activity uses phosphorylated exogenous FAs (green) produced by the FA kinase Fak (4), to produce FA-ACP. FASII inhibition (dashed red T) is bypassed by exogenous FAs (6), which are converted to FA-$PO_4$ and used to fill position 1 *via* PlsY, and position 2 by reverse PlsX activity, to produce PA. In a Δ*plsX* mutant, FAs charging position 1 are exogenous, while those charging position 2 are FASII-synthesized; in this case, the two FA sources are disconnected. See (1, 6, 9, 12) for references. Enzymes circled in grey are not discussed in this study.

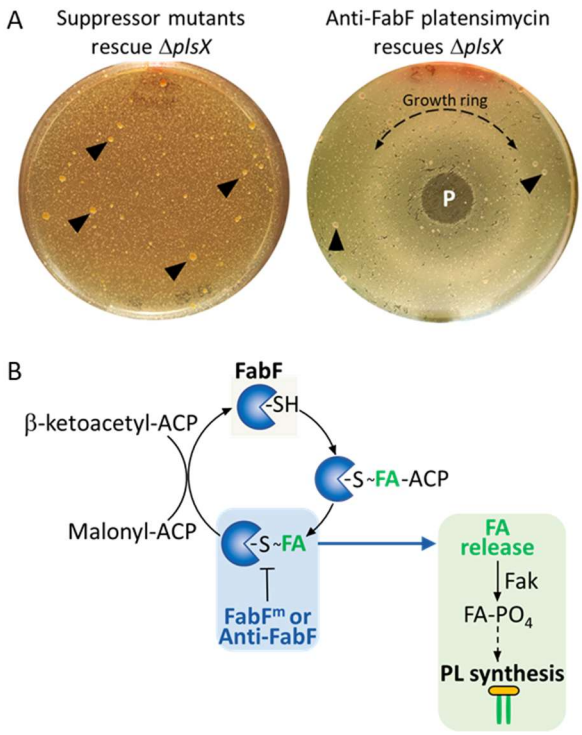


**Fig. 2. *fabF* mutants or the FabF inhibitor platensimycin rescues Δ*plsX* growth in the absence of exogenous FAs. A.** Lawns of RN-R Δ*plsX* were spread on BHI medium without FA addition, without (left) or with (right) 1.5 µg platensimycin (P) deposited in the center. Plates were photographed after 4 days at 37°C. Black arrowheads, examples of suppressors, some of which map to *fabF*. Dashed arrow, a homogenous growth ring surrounds the platensimycin spot. N=4. **B.** Model for Δ*plsX* growth rescue by a FabF mutation ($FabF^m$) or by partial FabF inhibition by platensimycin (anti-FabF). FabF perturbations would reduce enzyme processivity, such that the unstable FabF-FA intermediate releases FAs prior to second substrate malonyl-ACP loading, as needed to bypass the Δ*plsX* defect. FabF in blue; Fak in green. Symbols for FabF are based on (41).

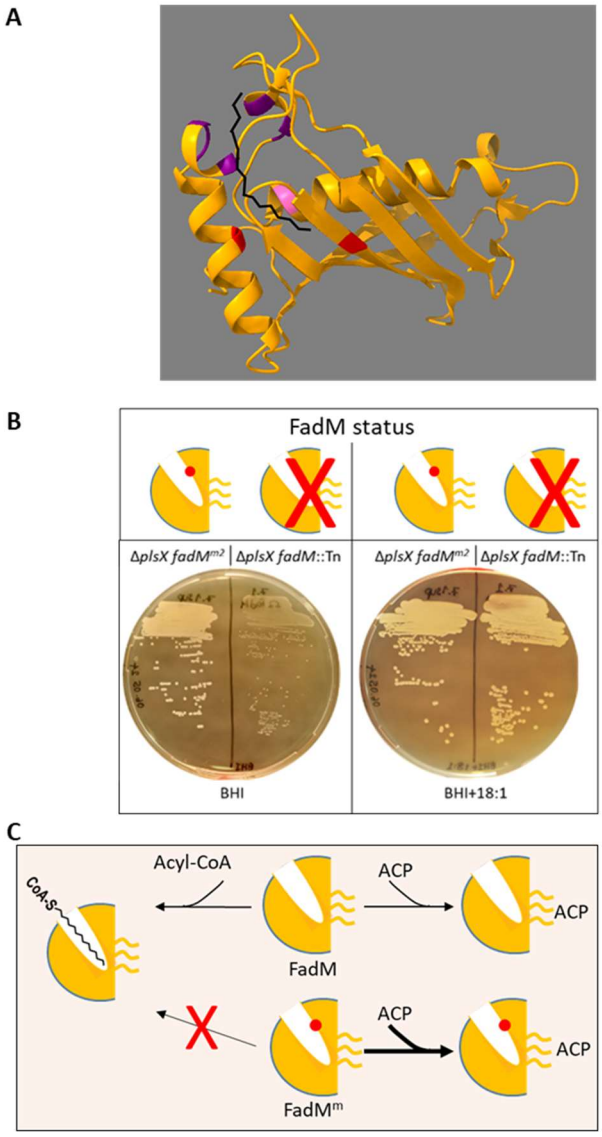


**Fig. 3. FadM mutations mapping to the FA binding tunnel, but not FadM inactivation, confer the *fadM* suppressor phenotype. A.** Schematized *S. aureus* FadM monomer binding to FA, based on crystal structure and Alphafold predictions ((18, 42), designed with https://alphafoldserver.com and http://www.cgl.ucsf.edu/chimera (43)). FA moiety (black line) binding in the FadM cavity requires amino acids Ile38 (pink), Tyr45; Met48, Leu122, Tyr125, and Phe126 (purple). The Δ*plsX* suppressors mapping to FadM affect amino acids Ile38Thr, Tyr90Phe, or Tyr133Phe (pink, and 2 red, respectively), which cluster around the FA-binding cavity; Ile38 (pink) is common to structural predictions and the identified suppressor. **B.** FadM inactivation abolishes Δ*plsX* suppression: Growth of Δ*plsX fadM*$^{m2}$ and the Δ*plsX fadM*::Tn derivative was compared on solid BHI medium without or with C18:1. Plates were photographed after 48 h growth at 37°C. Background growth on BHI (left) may be due to FA carryover from pre-cultures or to FA traces in medium. Plates are representative of biological triplicates. **C.** Model for FadM *versus* FadM$^{m}$ function. Binding of the acyl-CoA FA moiety in the FadM tunnel is needed for acyl-CoA TE activity. FadM mutations in the tunnel (red dot) diminish acyl-CoA – FadM interactions, reducing acyl-CoA TE activity but conserving ACP binding (thick arrow, right).

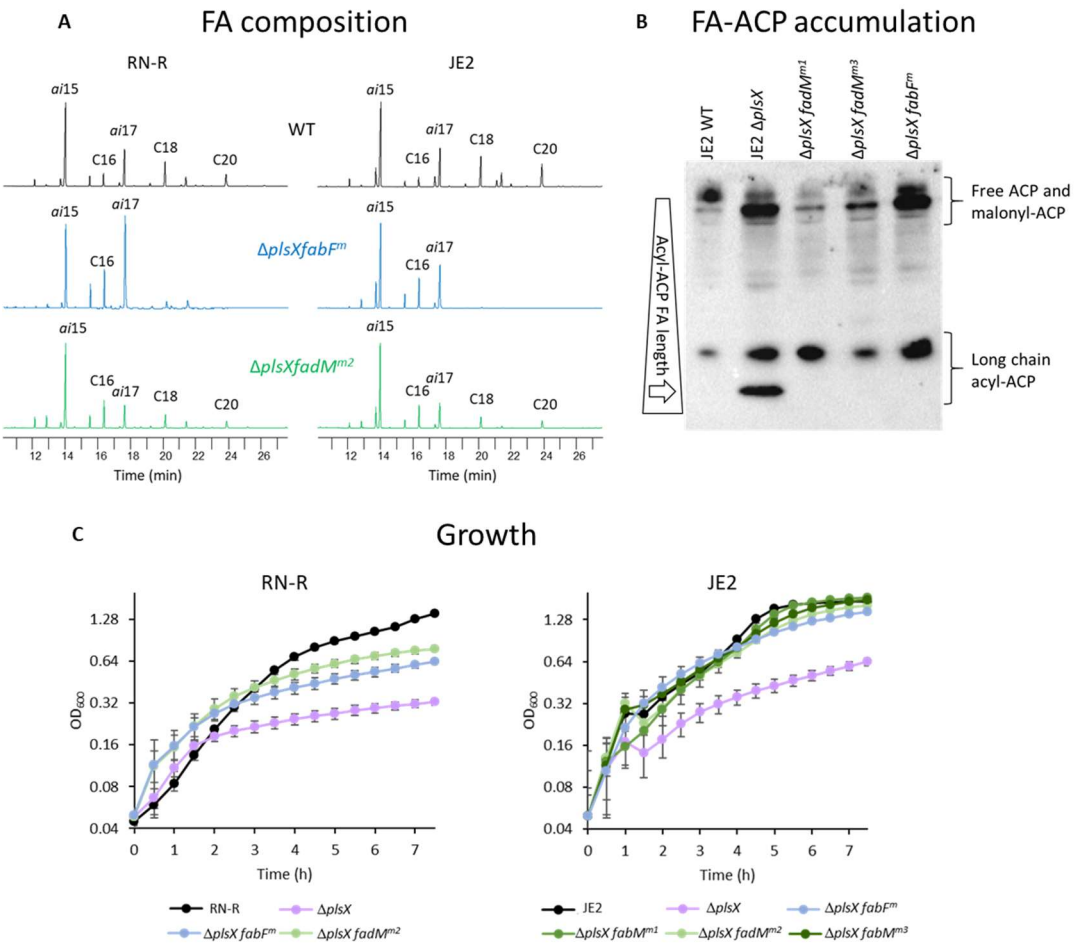


**Fig. 4. Behavior of *fabF* and *fadM* suppressors of Δ*plsX* without exogenous FAs. A.** FA profiles of RN-R (left)- and JE2 (right)- derived WT, Δ*plsX*, and *fabF* or *fadM* suppressors are extracted from BHI-grown cultures. FA assignments are as indicated. *ai*, anteiso; even numbered FAs are saturated (e.g., C16 is C16:0). The main FA component of WT *S. aureus* is *ai*15 (7). Peak heights correspond to relative responses (mV) of each FA in a sample. **Table S3** provides complete FA profile information. **B**. Acyl-ACP species in *S. aureus* JE2-derived Δ*plsX*, and Δ*plsX* suppressor strains. JE2 WT, Δ*plsX fadM*$^{m1}$, Δ*plsX fadM*$^{m3}$, and Δ*plsX fabF*$^{m}$ (using strains 7.5, 8.7, and 7.7, respectively; **Table S2**) were grown in BHI. The Δ*plsX* strain was grown in BHI+C18:1 medium, and shifted 2h to BHI prior to harvesting. Extracts were loaded on non-denaturing acrylamide gels, and immunoblotted using anti-ACP (7). Longer FA moieties on acyl-ACP migrate faster on gels (wedge; (29)). White arrow, accumulated acyl-ACP is not processed to phospholipids (5) (**Fig. 1**). Results are representative of biological duplicates. **C.** Growth of WT *S. aureus* (RN-R or JE2), Δ*plsX*, and Δ*plsX fabF* or Δ*plsX fadM* suppressors in BHI medium**.** Left: RN-R WT, and derivatives: Δ*plsX*, and Δ*plsX* suppressors encoding FabF$^{A119E}$ or FadM$^{Y90F}$ mutations (*fabF*$^{m}$ and *fadM*$^{m2}$ respectively). Right: JE2 WT, and derivatives: Δ*plsX*, and Δ*plsX* suppressors encoding FabF$^{A119E}$, FadM$^{I38T}$, FadM$^{Y90F}$, and FadM$^{Y133F}$ mutations (*fabF*$^{m}$, *fadM*$^{m1}$, *fadM*$^{m2}$, and *fadM*$^{m3}$, respectively). Mean and standard deviation of independent triplicate cultures are shown.

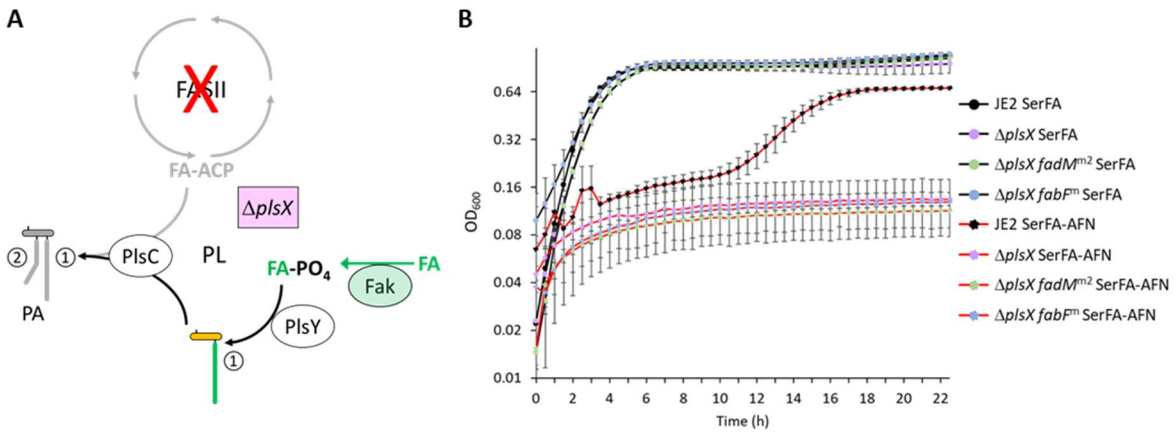


**Fig. 5. Synthetic lethal effect of a combined FASII and PlsX block. A.** Expected effects of FASII inhibition on an *S. aureus* Δ*plsX* mutant. In a WT strain, FASII inhibition by mutation or by antibiotic action is overcome by exogenous FAs, which are phosphorylated by Fak (4). FA-$PO_4$ is the substrate for PlsY and for reverse PlsX activities, and is thus used for phospholipid (PL) synthesis at both the 1 and 2 positions. If both FASII and PlsX are blocked as shown, exogenous FAs can only fill position 1. Thus either defect can be rescued separately by FA supplementation, but not the combination. Green, exogenous FAs and FA kinase; purple, *plsX* deletion; grey, pathways and products affected by combined FASII and PlsX block. **B.** Effects of anti-FASII treatment on JE2 Δ*plsX*, and Δ*plsX* suppressor strains in FA-supplemented medium. Strains were precultured in SerFA, and grown in SerFA without or with addition of 0.5 µg/ml anti-FASII AFN-1252 (SerFA-AFN). When the anti-FASII is added, WT *S. aureus* strains incorporate FAs to constitute membrane phospholipids, thus bypassing inhibition (6, 8, 44). As Δ*plsX* suppressors cannot generate FA-ACP needed for FASII bypass (6, 9, 12), they remain sensitive to anti-FASII. Mean and standard deviation of independent triplicate cultures are shown. Black lines, no anti-FASII, red lines with anti-FASII. *fadM*$^{m2}$ encodes FadM$^{Y90F}$; *fabF*$^{m}$ encodes FabF$^{A119E}$.

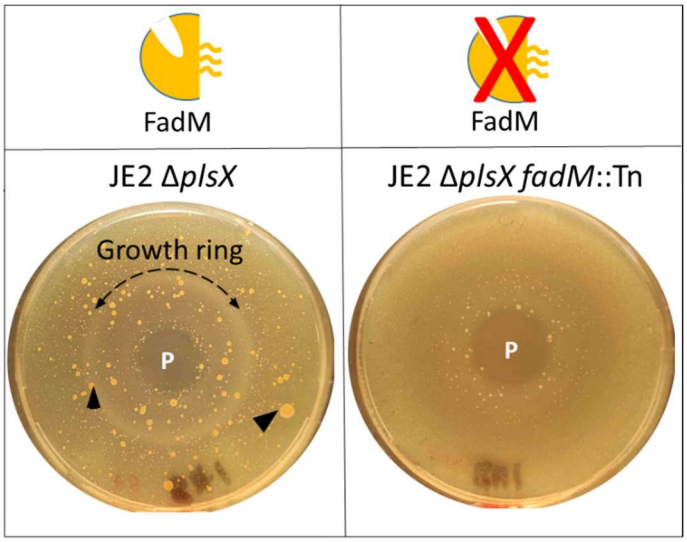


**Fig. 6. *fabF* suppressors of Δ*plsX* only arise when *fadM* is present.** FadM (depicted above) is present in JE2 Δ*plsX* (left) and absent in Δ*plsX fadM*::Tn (right, derived from strain 7.1: **Table S2**). Both strains were plated on BHI solid medium (100 µl of $OD_{600}$ = 0.005), and spotted with platensimycin (P; 1.5 µg). Plates were photographed after 6 days at 37°C. Black arrowheads point to Δ*plsX* suppressor clones. The dashed curved line indicates the growth ring surrounding platensimycin spotting. The small colonies surrounding platensimycin on Δ*plsX fadM*::Tn lawns (right) failed to regrow on BHI medium. Results are representative of 3 independent cultures and platings.

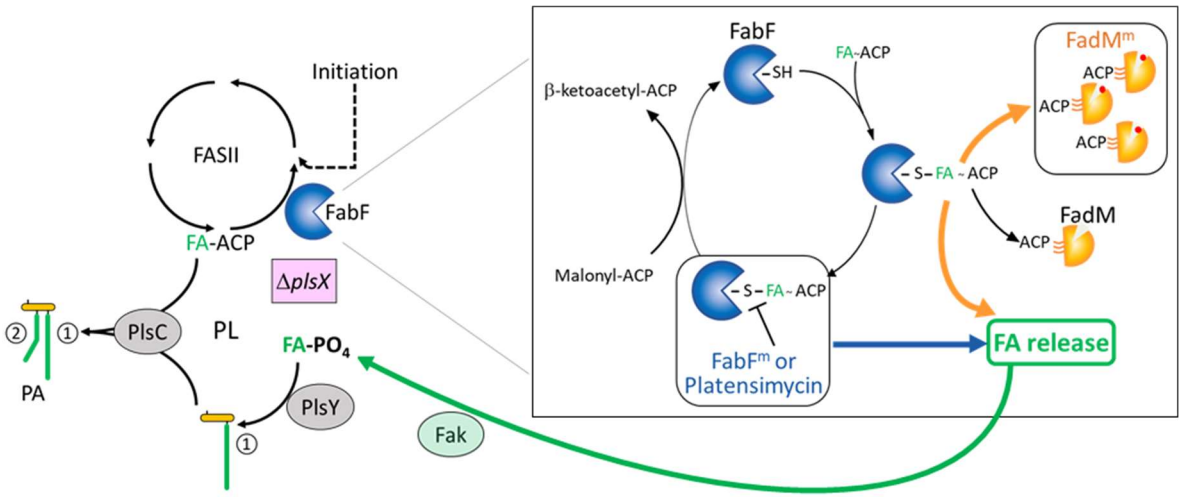


**Fig. 7. Proposed role of FabF - FadM interactions in controlling FA release and recycling from FabF intermediates.** Left, FASII and phospholipid synthesis coupled pathways. The *plsX* deletion dissociates the pathways, such that a free FA pool is required for survival. Symbols are as in Fig. 1. **Inset:** Model for FabF or FadM interactions that coordinately overcome Δ*plsX* growth arrest when either function is mutated. FabF (blue packman) catalyzes the first recursive step of FASII elongation: it cleaves acyl-ACP (FA-ACP) to release ACP, which then allows malonyl-ACP entry into the FabF cavity to extend the acyl intermediate by 2 carbons (17, 32). The $FabF^{A119E}$ mutant, or addition of anti-FabF inhibitor platensimycin, would prevent malonyl-CoA entry, leading to FA release (FA symbols in green). FadM (gold) is bifunctional, with acyl-CoA thioesterase (TE) and ACP binding activities (18, 20-22). Suppressor mutations in FadM ($FadM^m$ red dot) obstruct the FadM acyl binding cavity and hence acyl-CoA TE, increasing FadM availability for ACP binding (boxed $FadM^m$). Greater FadM-ACP binding would drive ACP release from the FabF pocket and favor leakage of FAs, which are then processed for phospholipid (PL) synthesis *via* FakA (4). Symbols for FabF are based on (41).

## Supplementary Figures and Tables

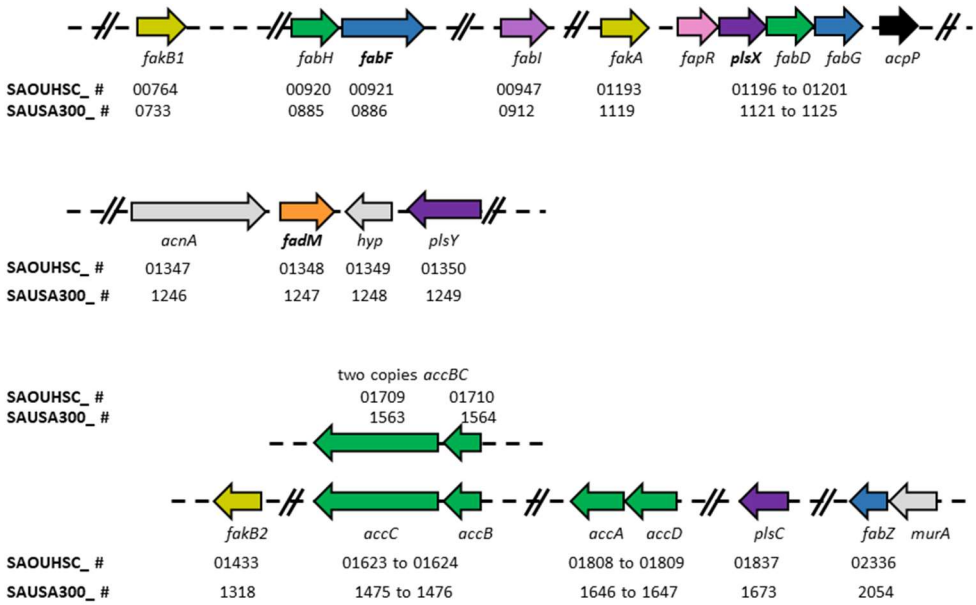


**Fig. S1. FASII and phospholipid gene organization in RN-R and JE2 strains.** *Orfs* related to this study are in bold. Dark green, FASII initiation; blue, FASII elongation; black, acyl carrier protein (*acpP*); purple, phospholipid synthesis; olive, FASII bypass fatty acid kinase; pink, regulatory; orange, FadM; grey, not directly related. Locus names are given for USA300 FPR_3797 (JE2) and 8325-4 (RN-R parent).

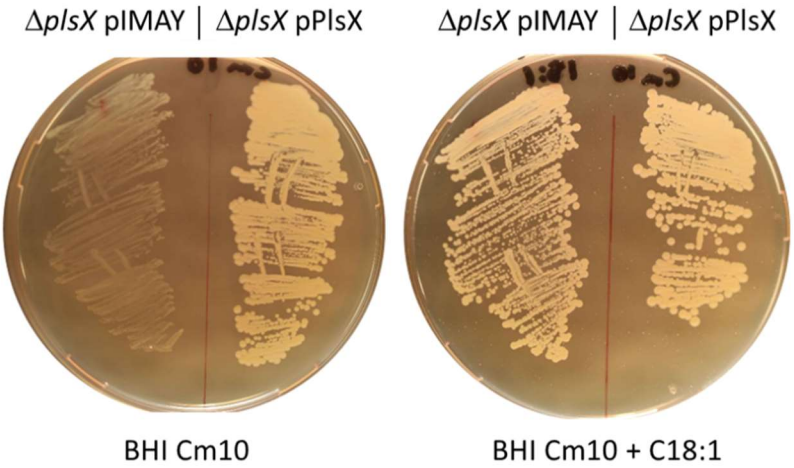


**Fig. S2. Complementation of Δ*plsX* by a plasmid-carried *plsX* gene.** RN-R Δ*plsX* strains containing an empty plasmid (pIMAY; left side of plates), or a plasmid carrying the *plsX* orf expressed from its native promoter on pIMAY (pPlsX; right side of plates), were streaked on BHI-chloramphenicol (Cm) 10 µg/ml solid medium without, or with C18:1 (250 µM) to bypass *plsX* absence. Background growth on BHI (left) may be due to FA carryover from pre-cultures or to FA traces in medium. Plates were photographed after 48h growth at 30°C. The Δ*plsX* strain carrying the empty plasmid failed to grow in the absence of C18:1 supplementation, while the pPlsX-complemented strain grew in both media.

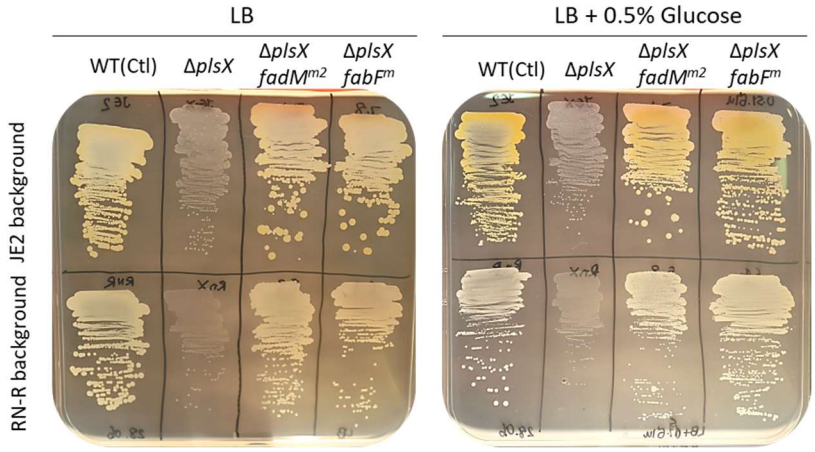


**Fig. S3. FadM$^m$ acyl-CoA thioesterase activity is not needed for Δ*plsX* suppression. A.** The FadM$^m$ suppressor phenotype is not subject to glucose repression, suggesting that Fad-mediated acyl-CoA synthesis is not involved. FA degradation (Fad) enzyme FadE converts FA to acyl-CoA, a FadM substrate (18). The *fad* operon is subject to CcpA-glucose repression (24, 25), suggesting that acyl-CoA pools would drop in glucose-containing medium. Strains precultured in LB and LB with C18:1 for Δ*plsX* (Materials and Methods) were streaked directly on solid LB medium with or without 0.5% glucose. Background growth on LB (left) may be due to FA carryover from pre-cultures. Upper and lower rows, strains are derived from JE2 and from RN-R, respectively. Results represent biological triplicates.

**Table S2. Δ*plsX* suppressors [a,b].**

| | **Gene : protein mutations in Δ*plsX* suppressor mutants** | | | | |
|---|---|---|---|---|---|
| | SAUSA300_0886 FabF (3-oxoacyl-ACP synthase II) | | SAUSA300_1247 FadM (acyl-CoA TE/ACP-binding (18, 20-22)) | | |
| Strain name | *fabF*$^{m}$: FabF$^{A119E}$ | *fabF*$^{m2}$: FabF$^{D266A}$ | *fadM*$^{m1}$: FadM$^{I38T}$ | *fadM*$^{m2}$: FadM$^{Y90F}$ | *fadM*$^{m3}$: FadM$^{Y133F}$ |
| RN4220 5.1 | X | | NT | NT | NT |
| RN4220 5.2 | X | | NT | NT | NT |
| RN4220 5.3 | X | | NT | NT | NT |
| RN4220 5.4 | X | | NT | NT | NT |
| RN4220 5.5 | X | | NT | NT | NT |
| RN4220 5.6 | | | | X | |
| **RN4220 5.7** | | | | **X** | |
| RN4220 5.8 | | | | X | |
| RN4220 6.1 | X | | NT | NT | NT |
| RN4220 6.2 | X | | NT | NT | NT |
| RN4220 6.3 | X | | NT | NT | NT |
| RN4220 6.4 | X | | NT | NT | NT |
| RN4220 6.5 | X | | NT | NT | NT |
| RN4220 6.6 | X | | NT | NT | NT |
| RN4220 6.7 | | | | X | |
| RN4220 6.8 | X | | NT | NT | NT |
| **JE2 7.1** | | | | **X** | |
| JE2 7.2 | | | X | | |
| JE2 7.3 | | | | X | |
| JE2 7.4 | | | X | | |
| **JE2 7.5** | | | X | | |
| JE2 7.7 | X | | NT | NT | NT |
| JE2 7.8 | X | | NT | NT | NT |
| JE2 8.1 | | | X | | |
| JE2 8.2 | | | | X | |
| JE2 8.3 | | | X | | |
| JE2 8.4 | | | X | | |
| JE2 8.5 | | | X | | |
| JE2 8.6 | | | X | | |
| JE2 8.7 | | | | | X |
| JE2 8.8 | | | | | X |
| **JE2 Sup1 [b]** | X | | | | |
| **JE2 Sup2 [b,c]** | | X | | | |

[a] 'X' indicates that the mutation is present in the tested isolate. NT, not tested; without indication, no mutation detected by DNA sequencing. Suppressors identified from whole genome sequencing are in bold. [b] Sup1 and Sup2 suppressors of Δ*plsX* had the same secondary mutation in SAUSA300_100 (generating Csa1A$^{K185Q}$), which was absent in subsequently isolated suppressors mapping to *fabF*. [c] Sup2, encoding FabF$^{D266A}$, could not be propagated after storage.

[b] **Accompanying Excel Table S1. Sequence comparisons of Δ*plsX* suppressors and reference strains.**

**Table S4. Genetic materials.**

| Strains | | | |
|---|---|---|---|
| **Host strain** | **Strain** | **Description** | **Reference** |
| JE2 USA300_FPR3757 | JE2 (WT) | USA300_FPR3757 cured of its three native plasmids | (25) |
| | Δ*plsX* | In-frame *plsX* deletion leaving operon intact | This study |
| | Δ*plsX* suppressor in *fadM*; *ΔplsXfadM*$^{m1}$ | *fadM*$^{m1}$ encodes FadM$^{I38T}$ | This study |
| | Δ*plsX* suppressor in *fadM; ΔplsXfadM*$^{m2}$ | *fadM*$^{m2}$ encodes FadM$^{Y90F}$ | This study |
| | Δ*plsX* suppressor in *fadM; ΔplsXfadM*$^{m3}$ | *fadM*$^{m3}$ encodes FadM$^{Y133F}$ | This study |
| | Δ*plsX* suppressor in *fabF; ΔplsXfab*$^{m}$ | *fabF*$^{m}$ mutant encodes FabF$^{A119E}$ | This study |
| | *fadM* Tn insertion | JE2 derivative containing an erythromycin-resistance-marked transposon (Tn) insertion in SAUSA300_1247 at position 1384915 (based on JE2 genome entry NZ_CP020619) | (25) |
| | Δ*plsX fadM*::Tn | Φ80 phage transduction of the SAUSA300_1247 Tn insertional mutant into the Δ*plsX fadM*$^{m2}$ (7.1) suppressor | This study |
| RN-R 4220 | RN-R 4220 (WT) | RN4220 derivative repaired for *fakB1* | (15) |
| | Δ*plsX* | In-frame deletion of *plsX* leaving operon intact | This study |
| | Δ*plsX* suppressor in *fadM; ΔplsXfadM*$^{m2}$ | *fadM*$^{m2}$ mutant encodes FadM$^{Y90F}$ | This study |
| | Δ*plsX* suppressor in *fabF; ΔplsXfabF* | *fabF* mutant encodes FabF$^{A119E}$ | This study |
| **Plasmids** | | | |
| | **Plasmid** | **Description** | **Reference** |
| | pMAD | Thermosensitive plasmid used to generate double-crossover deletion events | (35, 36) |
| | pMAD::*fapR-fabD* fragments | Used to generate *plsX* deletion | This study |
| | pIMAY | Used for *plsX* cloning | (37, 45) |
| | pIMAY::*plsX* | Used for *plsX* complementation in Δ*plsX* | This study |
| **Transducing phage** | | | |
| | **Phage** | **Description** | **Reference** |
| | ϕ80 | Used to transduce erythromycin-resistance-marked Tn insertion of SAUSA300_1247 into Δ*plsXfadM*$^{m2}$ background | (46) |

**Table S5. Oligonucleotides (5' to 3') used for genetic constructions and mutant detection**.

| Construction type and primers used for detection | | Description |
|---|---|---|
| **Plasmid for Δ*plsX* construction on pMAD linearized by SmaI** | | |
| pMAD_FapR_F | TCTATCGATGCATGCCATGGTACCCCTTCATCACAGACCATGAACTAAGC | *fapR* fragment |
| FapR_FabD_R | CGGAAAAATAATTGCTGTTTTACTCATAATTTTATCCTCGCTTATCATAAAAC | |
| FapR_FabD_F | GTTTTATGATAAGCGAGGATAAAATTATGAGTAAAACAGCAATTATTTTTCCG | *fabD* fragment |
| FabD_pMAD_R | GCAGAAGCTTCTAGAATTCGAGCTCCCTGTGACCTGAAACAACAATTTGACC | |
| **Verifications for pMAD constructions** | | |
| pMAD_F | GTTACGTTACACATTAACTAGACAG | |
| pMAD_R | TGGACAGCATGGCCTGCAACGC | |
| **Cloning *plsX* on pIMAY-derived locus1 plasmid** | | |
| pIMAY_FapR_F | AGTTTGTGGTTTAATGGGGTTGACACTTGAACTATTTAAA | *fapR* fragment |
| FapR_PlsX_R | TCAATTGCTAATTTAACCATTTTTTAGTACCTAGTCTTAA | |
| FapR_PlsX_F | TTAAGACTAGGTACTAAAAAATGGTTAAATTAGCAATTGA | *plsX* fragment |
| plsX_pIMAY_R | TTGTTGCTATAATGAAATGCGTTCTTACTCATTTGATTCACCTA | |
| pIMAY_FapR_R | TTTAAATAGTTCAAGTGTCAACCCCATTAAACCACAAACT | pIMAY linearized by reverse PCR |
| plsX_pIMAY_F | TAGGTGAATCAAATGAGTAAGAACGCATTTCATTATAGCAACAA | |
| **Δ*plsX* suppressor verifications** | | |
| FabF_F | GGAATCAGCTAGAGAACGC | SAUSA300_0886 |
| FabF_R | CATTTTTCAACCCACAAGAGG | |
| 1247_F | AATCGGTATTTGAGGCAC | SAUSA300_1247 |
| 1247_R | ATCTTCACGCTAATTACATT | |
| 0100_F | CGTGGCCTGGATATGATGAT | SAUSA300_0100 *csa1* |
| 0100_R | GATTATCCTGAGCTACTTCG | |
| **Verifications of Tn insertion in SAUSA300_1247** | | |
| 1247_F | GGATTACTATCGTCACGGTGG | Transposon insertion |
| UpBursa_F | CTCGATTCTATTAACAAGGG | |